In-vivo soft tissue NMR imaging of the rat thorax and abdomen[1]

P.A. Bottomley[2]

Department of Physics, University of Nottingham, University Park, Nottingham NG7 2RD (England), 8 May 1980

Summary. An in vivo study of the anatomy of the thorax and abdomen of a rat by proton sensitive-line NMR imaging is presented and a contrast mechanism for soft tissue differentiation in images discussed.

An NMR image or 'zeugmatogram'[3] is a 2- or 3-dimensional plot which maps the spatial distribution of the NMR signal in some generally heterogeneous specimen. Applications of NMR imaging methods to the study of biological and medical organisms is of potential value since NMR imaging methods a) are noninvasive, b) utilize naturally abundant nuclear species to generate signals, thus obviating the need for artificial image enhancement agents such as radiopharmaceuticals or X-ray opaque dyes, c) use no ionizing radiation and moreover have no known associated hazard[4,5] d) are completely automated requiring no moving parts or rotating gantries[6], and most importantly e) the image intensity, which is a function of the NMR relaxation times and nuclear spin density, is a high contrast parameter providing good differentiation of the normal and pathological tissues thus far investigated[6–10].

Since the production of the 1st NMR images on a small 4 mm sized system in 1972[3], a variety of different NMR imaging methods have been proposed[11], and larger scale systems constructed for small animal, human limb[12], and most recently, human head imaging[13]. Examples of NMR imaging studies undertaken with an 8 cm aperture instrument which employs the novel 'sensitive line' method include series of scans through a rabbit head, the human hand and forearm in-vivo, and an in-vivo study showing the detection and development of a tumour in the abdomen of a rat[6–8]. A survey and comparison of these and other NMR imaging results has recently been prepared[14]. An in-vivo proton sensitive-line NMR imaging study of the abdomen and thorax of a rat is presented here.

Method. Details of the sensitive-line method appear elsewhere[15]. A qualitative understanding may be obtained from a consideration of the Larmor equation $\omega_0 = \gamma H_0$ which defines the sharp resonance frequency ω_0 of spin-possessing nuclei subject to a uniform applied magnetic field H_0. Such nuclei are common and include for example isotopes

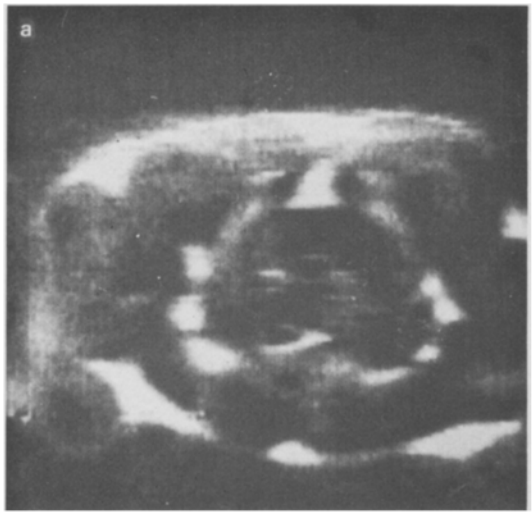

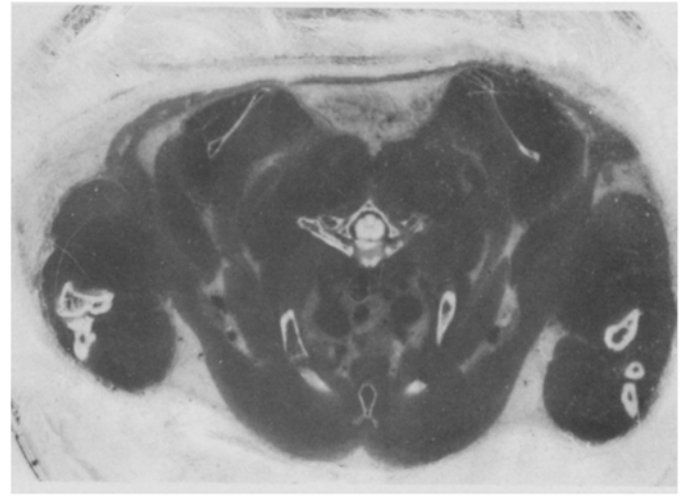

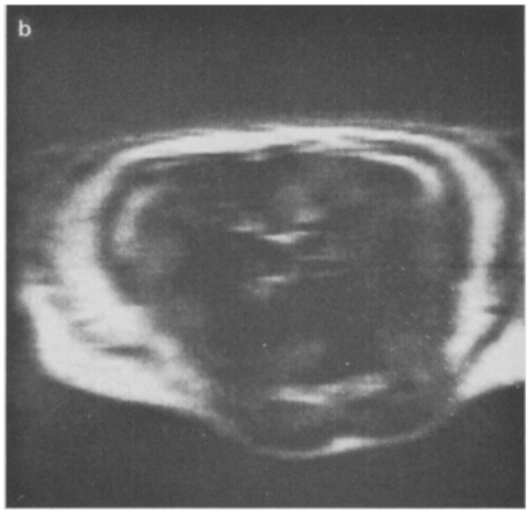

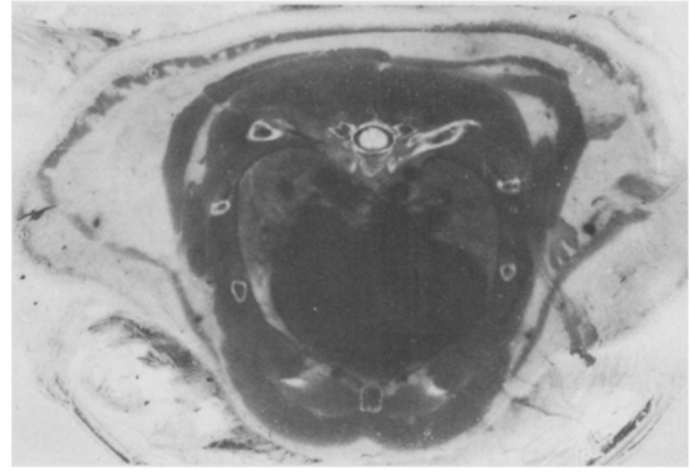

of hydrogen, carbon, phosphorus, fluorine, nitrogen, and oxygen, each with unique gyromagnetic ratios γ which enable them to be selected independently of each other[6]. Clearly if the magnetic field is not constant over the sample but has a linear gradient, say $H_0 = H_0(X)$ in the X direction, then the corresponding resonant response, $\omega_0 = \omega_0(X)$, is a spectrum which represents the distribution of nuclei in the X direction and is in fact a 1-dimensional projection or image in that direction. Resolution of spatial information in the remaining 2 dimensions is achieved by application of 2 additional magnetic field gradients which are time-dependent and mutually orthogonal. Time-dependent gradients of the form $(Y\text{-}Y_0)g_Y \cos(\Omega_Y t)$ and $(Z\text{-}Z_0)g_Z \cos(\Omega_Z t)$, where Y, Z, t, g_Y, g_Z, Ω_Y, and Ω_Z are respectively the orthogonal cartesian and the time coordinate parameters and the gradient amplitudes and angular frequencies, contribute non-zero fluctuations to the resonant response from all of the sample except for the region $Y = Y_0$, $Z = Z_0$ where these gradients vanish. Removal of the time-dependent contributions by signal averaging results in an NMR-spectrum which corresponds to the sample distribution along the sensitive line at (X, Y_0, Z_0). The sensitive line is scanned sequentially across the imaging plane to yield a cross-sectional image and the data is simultaneously displayed as intensity on an oscilloscope screen.

Results and discussion. The figure presents a series of NMR image scans through a live sedated 700 g Sprague rat, as compared with subsequent corresponding postmortem anatomical sections of the animal. All images consist of 128×128 independent pixels of approximately 3 mm $\times$ 0.4 mm $\times$ 0.4 mm size and were obtained in total imaging times of 640 sec. A steady-state free precession NMR pulse sequence at a 30 MHz proton resonance was employed. The gradient frequencies and amplitudes were 20 Hz and about 10^{-2} T/m respectively. Some distortion in the shape of the anatomical sections and errors in determining the exact location of the image plane resulted during the sectioning procedure.

The principal feature in these images is adipose tissue which generates a strong NMR signal and appears white, in contrast to muscle and vital organs which appear dark, and the stomach and intestine which appear grey and heterogeneous in structure. This is because the observed NMR signal is approximately proportional to the ratio $R = 2T_2 \cdot (T_1 + T_2)^{-1}$ where T_1 and T_2 are the longitudinal and transverse relaxation times respectively[6,8,15]. Since $T_2 \leq T_1$, $R \leq 1$. Assuming published proton relaxation time data on excised mice and human samples in the range 15 to 30 MHz[16], the value of R for adipose is 0.88 compared with values of 0.21, 0.18, 0.16, 0.14, 0.13, 0.12, and 0.11 for stomach, intestine, kidney, lung, heart, liver, and muscle respectively. Alternative pulse sequences will alter the relative contrast and intensities in a manner dependent upon the tissue relaxation times. Note the absence of

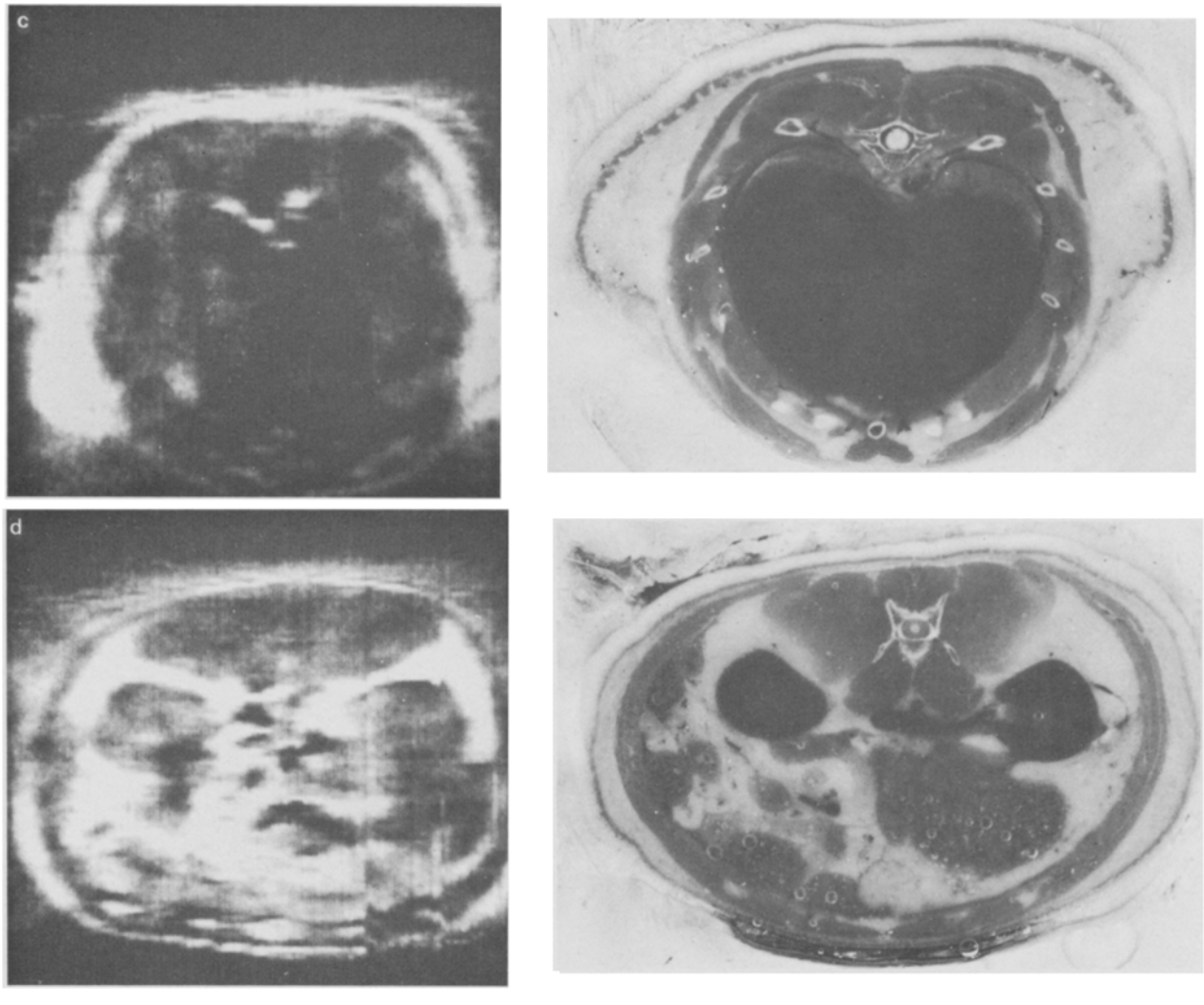

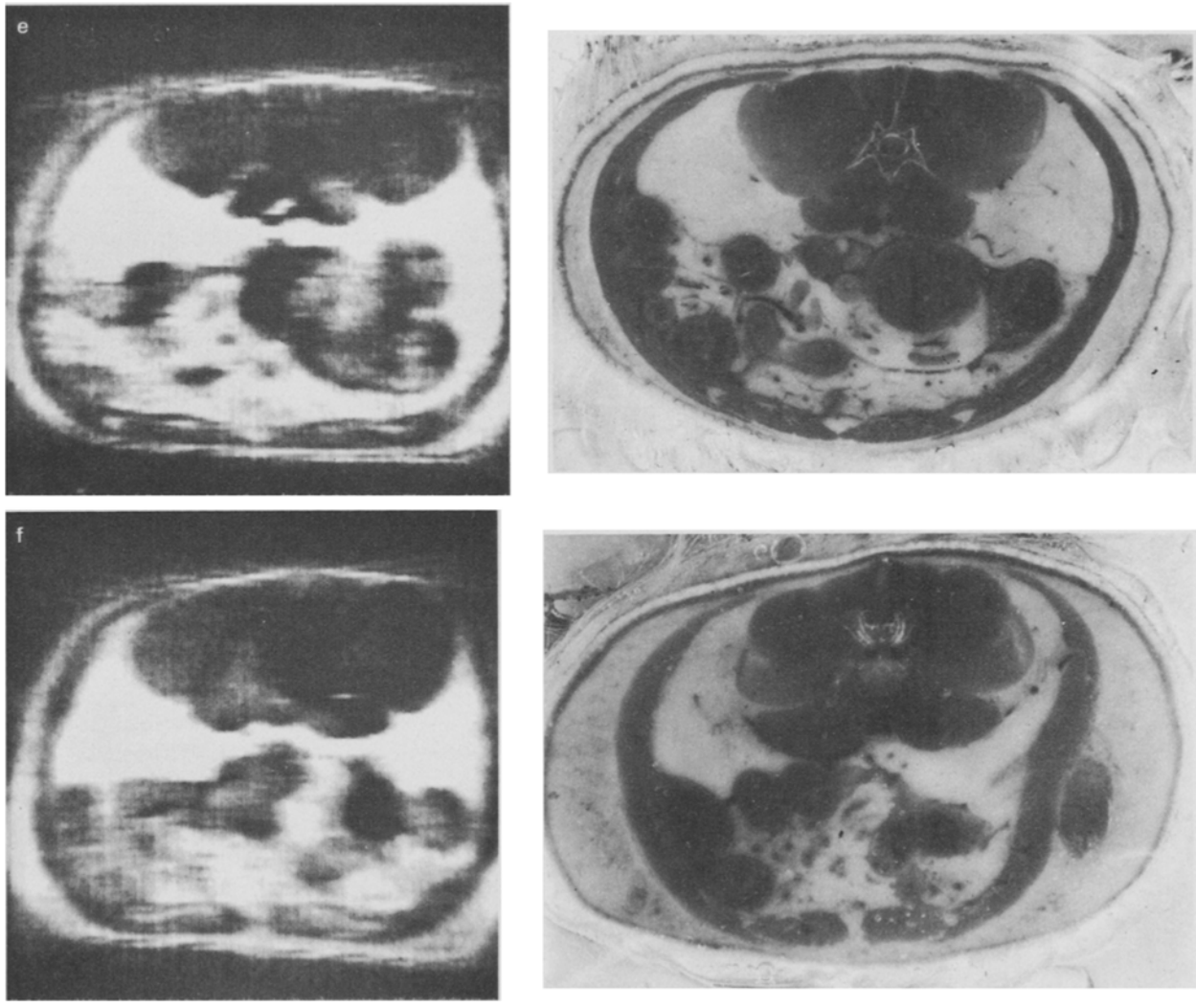

NMR images (left) and corresponding post-mortem anatomic sections (right) of a rat. Images are oriented dorsal surface uppermost looking towards the tail. *a* Is through the lungs immediately above the heart; *b* intersects the heart and lungs; *c* is through the median and lateral lobes of the liver; *d* intersects the kidneys and *e* and *f* are successively lower sections through the abdomen showing the intestinal tract and the colon.

motion induced artefacts generated by natural involuntary physiological functions in this method of imaging. Abrupt vertical lines in the image of figure d were produced by the animal twitching during the experiment.

Conclusion. Good quality transverse-section anatomical NMR images of the rat trunk can be obtained in periods of about 10 min. The contrast between soft tissues in the images is attributed mainly to differences in the characteristic NMR relaxation times. Extrapolation of the results to human trunk experiments at 5 MHz suggest imaging times of order 1 min if the array size and some other experimental parameters are held constant[14]. Soft tissue differentation may also be enhanced at 5 MHz due to the frequency dependence of the relaxation times[17].

1 Acknowledgment. I thank E.R. Andrew, W.S. Hinshaw, G.N. Holland, W.S. Moore, and C. Simaroj for their valuable contributions, and the MRC for financial support.
2 Present address: General Electric Company, Research and Development Centre, P.O. Box 8, Schenectady, N.Y., USA.
3 P.C. Lauterbur, Nature *242*, 190 (1973).
4 P.A. Bottomley and E.R. Andrew, Physics Med. Biol. *23*, 630 (1978).
5 T.F. Budinger, IEEE Trans. nucl. Sci. *NS-26*, 2821 (1979).
6 W.S. Hinshaw, E.R. Andrew, P.A. Bottomley, G.N. Holland, W.S. Moore and B.S. Worthington, Br. J. Radiol. *51*, 273 (1978); *52*, 36 (1979).
7 W.S. Hinshaw, P.A. Bottomley and G.N. Holland, Nature *270*, 722 (1977); Experientia *35*, 1268 (1979).
8 P.A. Bottomley, Cancer Res. *39*, 468 (1979).
9 I.L. Pykett and P. Mansfield, Physics Med. Biol. *23*, 961 (1978).
10 P. Mansfield, P.G. Morris, R. Ordidge, R.E. Coupland, H.M. Bishop and R.W. Blamey, Br. J. Radiol. *52*, 242 (1979).
11 P. Mansfield, Contemp. Phys. *17*, 553 (1976); D.I. Hoult, J. magn. Reson. *33*, 183 (1979).
12 E.R. Andrew, P.A. Bottomley, W.S. Hinshaw, G.N. Holland, W.S. Moore and C. Simaroj, Physics Med. Biol. *22*, 971 (1977).
13 G.N. Holland, W.S. Moore and R.C. Hawkes, J. Computer Assist. Tomogr. *4*, 1 (1980).
14 P.A. Bottomley, J. magn. Reson. *36*, 121 (1979).
15 W.S. Hinshaw, J. appl. Phys. *47*, 3709 (1976); F.T. Meieire and F.C. Thatcher, J. appl. Phys. *50*, 4491 (1979).
16 H.E. Frey, R.R. Knispel, J. Kruuv, A.R. Sharp, R.T. Thompson and M.M. Pintar, J. natl Cancer Inst. *49*, 903 (1972); M. Goldsmith, J.A. Koutcher and R. Damadian, Br. J. Cancer *38*, 547 (1978).
17 G. Diegel and M.M. Pintar, J. natl Cancer Inst. *55*, 725 (1975); R.L. Nunnally and D.P. Hollis, unpublished data (1976).